heat flux by both radiation and conduction should be twice as much in the half-scale model as in the prototype. Since temperature differences between homologous foils must be the same in both model and prototype, the increased fluxes in the model must be provided by increased emissivity and conductance in the model. The emissivity is easily increased by such means as black dots on the surface, but accurate changes to the conductance would be much more difficult. The model foil may not actually need to be thinner, since the temperature drop across each foil is usually neglected; and this need not necessarily introduce distortion if the increased model conductance is to be obtained by greater compression of the model MLI. However, the uncertainty in conductance values is large enough, especially when different means of construction are used, that this method is actually less attractive than the more convenient one discussed previously.

To summarize, surface control techniques allow thermal modeling of MLI without geometric distortion or modification of the foil used to build up the MLI, except the surface emissivity of the outermost layer, where normal scaling laws again control the emissivity. Both temperature and material can be preserved, provided the number of layers of foil on the prototype is an integral multiple of $1/R$, the reciprocal of the scale ratio.

References

[1] Gabron, F., "Thermal Scale Modeling Techniques for Voyager-Type Spacecraft," Rept. 951417, Arthur D. Little Inc., Cambridge, Mass.

[2] Shih, C., "Thermal Similitude of Manned Spacecraft," AIAA Paper 66-22, New York, 1966.

Newtonian Aerodynamic Coefficients for an Arbitrary Body, Including "All Shadowed" Areas

MELVIN L. ROBERTS*
General Electric Company, Cincinnati, Ohio

Introduction

NEWTONIAN hypersonic aerodynamic theory, based on the assumption of a thin shock layer, has been widely used because of its inherent simplicity. The main assumption is that local pressure coefficient C_p, varies only with local body angle of attack, θ, as long as the freestream can impinge directly on the point in question. Where the local point does not "see" the flow, $C_p = 0$. Applying these two concepts is straightforward and forms the basis of most applications today. The principal computational difficulty in making Newtonian calculations arises when one part of the body with $\theta < 90°$ is shielded from the freestream (shadowed) by a portion of the body upstream of it. In previous work this problem has either been ignored,[1] or has been solved by requiring that the body be specified by a series of mathematical surfaces bounded by space curves.[2] A simpler approach was sought, in which the body could be described by a series of planar cross sections, and each defined by a finite number of points. A technique has been developed for rapidly determining whether each body point is "shadowed" and for determining unambiguously the elemental surface areas, and associated local body normals.

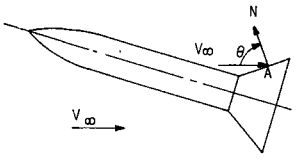

Fig. 1 Shading of a point by body upstream.

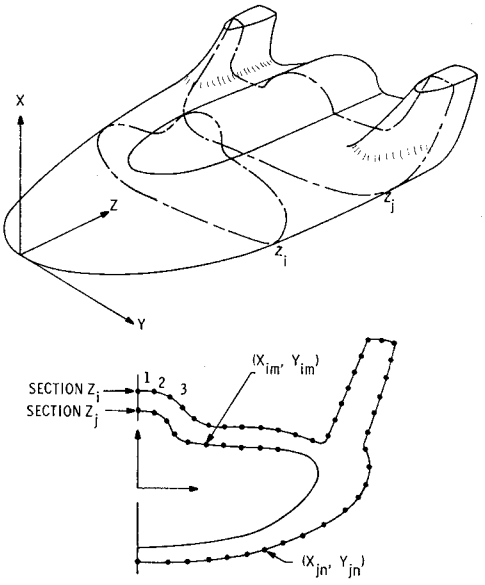

Fig. 2 Arbitrary body definition.

Shadow Area Determination

The basic equation of Newtonian flow theory $C_p = K \cos^2\theta$ yields the local C_p in terms of θ and a constant K, a function of Mach number. This equation is valid only for surface areas that "see" the flow (Fig. 1), for which $|\theta| \leq 90°$, where $\cos\theta = -\mathbf{V}_\infty \cdot \mathbf{n}/|V_\infty|$, $\mathbf{V}_\infty$ = freestream velocity vector, and $\mathbf{n}$ = local normal unit vector. For simple shapes (sphere, ellipsoid, cone, etc.) the shadow areas that don't "see" the flow, (for which $C_p = 0$) are determined simply by $|\theta| > 90°$. For more complex shapes, typified by flared bodies of revolution or complex lifting re-entry vehicles, a point on the surface may have $|\theta| < 90°$ and yet have $C_p = 0$ because it is shadowed by an upstream portion of the body, e.g., point A of Fig. 1.

Let us define the body in a Cartesian coordinate system (Fig. 2) by transverse sections normal to the z axis (z_i,z_j, etc.), and points in each cross section (x_{im},y_{im}), (x_{jn},y_{jn}), etc. In

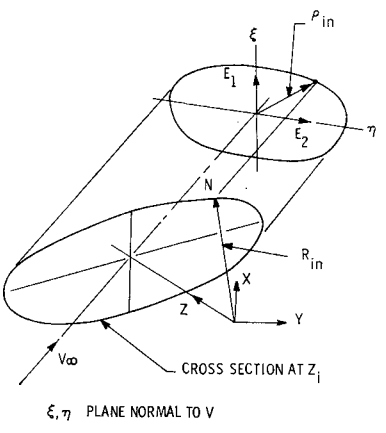

Fig. 3 Projection of z_i cross section onto ξ,η plane.

Received January 26, 1970, revision received April 27, 1970. Work done at General Electric Re-entry and Environmental Systems Division, Philadelphia, Pa.

* Design Analysis Engineer, Advanced Engineering, Aircraft Engine Technical Division. Member AIAA.

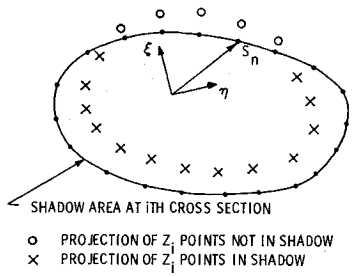

Fig. 4 ξ,η plane projection of z_i section with shadow cast by body upstream of z_i.

vector notation each body point is defined by a radius $\mathbf{r}_{im} = \mathbf{i}x_{im} + \mathbf{j}y_{im} + \mathbf{k}z_{im}$.

To define the shadow area we must start at the origin and successively project each cross section on to a ξ,η plane normal to $\mathbf{V}_\infty$ (Fig. 3). The shadow cast on the more aft cross sections by the forward portions of the body can be built up progressively, and the $\mathbf{r}_{im}$ body points in each cross section can then be tested as follows to determine whether they are shadowed. In Fig. 3, $\mathbf{r}_{in}$ defines the nth point (x_{in},y_{in}) in the ith cross section ($z = z_i$). Projected onto the ξ,η plane, normal to $\mathbf{V}_\infty$, this determines a vector $\boldsymbol{\varrho}_{in}$ in the ξ,η plane: $\boldsymbol{\varrho}_{in} = \mathbf{e}_1\xi_{in} + \mathbf{e}_2\eta_{in}$, where $\mathbf{e}_1$, $\mathbf{e}_2$ are unit vectors along ξ,η axes. The ith cross section, at $z = z_i$, is thus represented in the ξ,η plane by a set of vectors $\boldsymbol{\varrho}_{in}$, defining the points on a closed contour.

A point $\mathbf{r}_{in}$ on the body will be shadowed if its projection $\boldsymbol{\varrho}_{in}$ in the ξ,η plane lies within the projection of the previously determined shadow on the ξ,η plane. Now let the latter shadow be a series of points defined by the vectors $\mathbf{S}_n$, $n = 1, 2, 3, \ldots$, (Fig. 4). The closed contour defining the shadow is explicitly defined by the straight line segments connecting successive points.

The test for determining whether a point lies inside or outside a closed contour S is shown in Fig. 5. Consider a point P lying outside the contour S (Fig. 5a). Choosing an initial point 0 defines a vector **P0**. Now let the tip of this vector move along the contour of S, through points 1, 2, . . ., 6 and back to 0. The vector to any point, e.g., **P1** to point 1, makes an angle ϕ with **P0**. If ϕ is positive counterclockwise, then ϕ will reach a positive maximum value for P4 tangent to S. Proceeding from 4 to 5 and 6, ϕ will decrease, reaching a maximum negative value at **P6** after which it will increase again, becoming zero as the tip moves from 6 to 0. Thus for a point P external to a contour S we can pick an initial point 0 on the contour and then let the tip of the vector from P to S make one circuit of the contour. The angle ϕ between the initial and final positions of the vector will be zero.

On the other hand, if the point Q lies inside the contour S (Fig. 5b), we choose an initial point 0 and vector **Q0**, when the tip of the vector makes one circuit around S and returns to 0, ϕ will decrease continuously from 0 to -2π. Thus, the angle ϕ between the initial and final positions of the vector will be -2π, providing a clear distinction between inside and outside points.

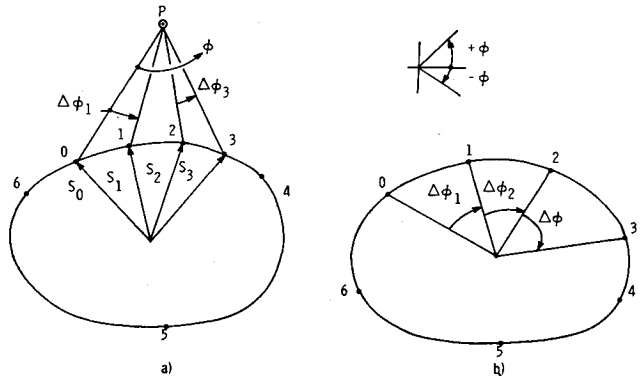

Fig. 5 Test for determining whether point is shadowed.

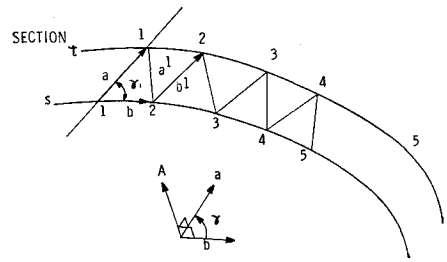

Fig. 6 Calculation of element of surface area and local normal vector.

For a shadow contour defined by a set of discrete points specified by vectors $\mathbf{S}_n$ ($n = 1, 2, 3, \ldots$), lines from P (or Q) are drawn to each of the n contour points. Each successive pair of points i and $(i + 1)$ define an angle $\Delta\phi_i$. We can let the tip of our vector from P (or Q) to S traverse the contour by summing all the $\Delta\phi_i$. Then,

$$\sum_{i=1}^{n} \Delta\phi_i = 0 \qquad \text{(P outside S)}$$

$$\sum_{i=1}^{n} \Delta\phi_i = -2\pi \qquad \text{(Q inside S)}$$

Thus for the ith cross section we can test each of the points $\boldsymbol{\varrho}_{in}$ in the ξ,η plane to determine whether or not it lies inside the shadow defined by the $\mathbf{S}_n$ and thus whether the original $\mathbf{r}_{in}$ are shadowed (Fig. 3). Furthermore, the shadow area cast on further aft sections can then be enlarged in a straightforward way to include the effect of the points of the ith cross section. Thus the shadow area can be built up by considering successive body cross sections.

Force Increment Calculation

Next, we compute the pressure distribution on the body surface between the $(i - 1)$st and ith cross sections. For the more complex shapes for which this technique is particularly applicable, complexities such as surface intersections, or saddle points, must be accommodated routinely, without the ambiguities that often arise when local surface elements are approximated by simple surfaces or sets of plane curves.

The basic technique for computing the area of, and local normal to, the elemental surface areas is shown in Fig. 6. Two successive cross sections are designated as s and t, and the points in each section are numbered sequentially around the cross section. In our vector notation, they would be defined by $\mathbf{r}_{s1}, \mathbf{r}_{s2}, \mathbf{r}_{s3}$ . . . in section s, and $\mathbf{r}_{t1}, \mathbf{r}_{t2}, \mathbf{r}_{t3}$ . . . in section t. Assuming that the pressure distribution on the body has been calculated up to section s, we wish to find the contribution of the body surface between sections s and t. We divide this surface into triangular facets as shown. Then, for the first triangle $s1$, $s2$, and $t1$ we compute $\mathbf{b} = \mathbf{r}_{s2} - \mathbf{r}_{s1}$ and $\mathbf{a} = \mathbf{r}_{t1} - \mathbf{r}_{s1}$. The area and normal vector to the segment are given by $\mathbf{A} = (\mathbf{b} \times \mathbf{a})/2$, where $|A| = (ab \sin\gamma)/2$ is the area of the segment. The direction of $\mathbf{A}$ determines the outward normal: $\mathbf{n} = \mathbf{A}/|A|$. Finally the force is assumed to act at the centroid of the area, given by $\mathbf{r}_A = (\mathbf{r}_{s1} + \mathbf{r}_{s2} + \mathbf{r}_{t1})/3$. Having $\mathbf{A}$, $\mathbf{n}$, and $\mathbf{r}_A$, we can find the Newtonian C_p and the contribution to the force and moment on the body We then proceed to the next triangular facet defined by points $s2$, $t1$, and $t2$ and let $\mathbf{b}' = \mathbf{r}_{t2} - \mathbf{r}_{s2}$, and $a' = \mathbf{r}_{t1} - \mathbf{r}_{s2}$, and so on.

To account for the possibility that one or more of the points defining a triangular segment may be in shadow, we assign a weighting factor W_{sm} to the point $\mathbf{r}_{sm}$

$$W_{sm} = \tfrac{1}{3}, \text{ if the point "sees" the flow}$$

$$W_{sm} = 0, \text{ if the point is in shadow}$$

Then for each triangular element we obtain a total weighting factor, similar to $W = W_{sm} + W_{s,m+1} + W_{tm}$ by adding the

weighting factors of the corners. W can take on the values 0, $\frac{1}{3}$, $\frac{2}{3}$, and 1, to account for either full, partial or no shadow on the triangular segment. The local pressure coefficient becomes $C_p' = WC_p = WK\cos^2\theta$.

A minor requirement imposed by the foregoing technique is that adjacent cross sections have the same number of defining points. Abrupt changes in cross section might require an increase in the number of points per section but this could be handled easily, by restarting the calculation at that section with more points per section.

References

[1] Gentry, Arvel E., "Hypersonic Arbitrary-Body Aerodynamic Computer Program, Mark III Version," DAC 61552, April, 1968, Douglas Aircraft Corp., Long Beach, Calif.

[2] Brong, E. A., and Matlin, S., "A Program for the Computation of Newtonian and Free Molecule Forces and Moments for Arbitrary Bodies," TIS 63SD210, Jan. 1963, General Electric Co., Reentry Systems Dept., Philadelphia, Pa.

A Ferry Package for Transporting Reusable Spacecraft and Launch Vehicles

THOMAS A. BLACKSTOCK*
NASA Langley Research Center, Hampton, Va.

Nomenclature†

C_L	= lift coefficient
C_l	= rolling moment coefficient; $C_{l_\beta} = \Delta C_l/\Delta\beta$
C_m	= pitching moment coefficient; $C_{m_\alpha} = \Delta C_m/\Delta\alpha$
C_n	= yawing moment coefficient; $C_{n_\beta} = \Delta C_n/\Delta\beta$
L/D	= lift-drag ratio
α,β	= angles of attack and sideslip, respectively
$\delta_a,\delta_e,\delta_r$	= aileron, elevon, and rudder deflections
Λ	= sweep angle

Introduction

THE concept of a reusable "space shuttle" capable of rapid turn-around offers promise of major reductions in the cost of space transportation. It would take off vertically with the first stage separating at a velocity of 9,000–15,000 fps and landing horizontally at a conventional landing field.

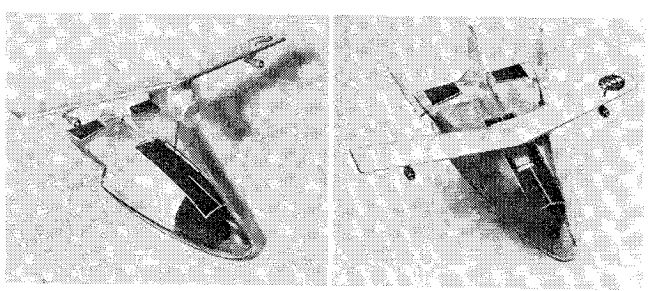

Fig. 1 HL-10 with ferry package.

Presented as Paper 70-259 at the AIAA Advanced Space Transportation Meeting, Cocoa Beach, Fla., February 4–6, 1970; submitted March 27, 1970; revision received May 21, 1970.

* Aerospace Engineer, Aerothermal Branch, Space Systems Research Division.

† The lateral data are referred to the body system of axes and the longitudinal data to the stability axes. The reference center of moments was located at 53% of the body length aft of the nose. All coefficients are based on body planform area, length, and span.

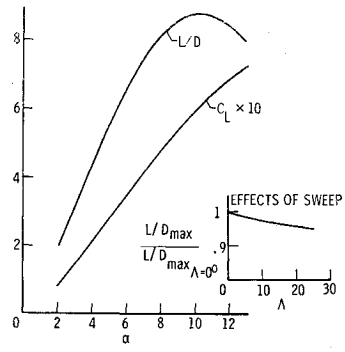

Fig. 2 Trimmed characteristics, HL-10 with ferry package with straight wing.

The second stage would continue into orbit with a capability of returning to Earth with or without cargo for a conventional horizontal landing. Ground rules under which NASA's recent preliminary contractual studies were conducted specified booster cruise-back to a field adjacent to the launch site. Normally the orbiter would also return to this site; however, other conditions dictated by mission and/or weather may necessitate landing elsewhere. In this event, the ability to ferry the vehicle from the landing site to the launch site is needed. To provide satisfactory cruise performance, higher subsonic L/D than is generally afforded by lifting bodies is desirable. Concepts employing fixed or extendable wings can provide this capability, but significant savings in gross lift-off weight are possible if only enough performance is provided to assure safe landing.

This Note deals with a proposal to increase subsonic L/D of the orbiter for ferry purposes through the use of a "ferry package" consisting of wings and engines attached to a fuel tank which is fitted into the vehicle cargo bay (Fig. 1). The concept is shown as it might be applied to the HL-10, a representative lifting body whose performance has been thoroughly studied in wind-tunnel and flight tests. The basic principles of this concept could be applied to most orbiters being considered in the current space shuttle studies. For those configurations whose subsonic L/D is satisfactory, engines and fuel tanks might constitute the total unit.

Aerodynamic Characteristics

Aerodynamic characteristics of ferry configurations with straight and swept wings of aspect ratio 10 are shown in Figs. 2 and 3 as obtained from tests at a Mach number of 0.3 and Reynolds numbers up to 15×10^6 based on body length. The results shown summarize curves of trimmed performance and

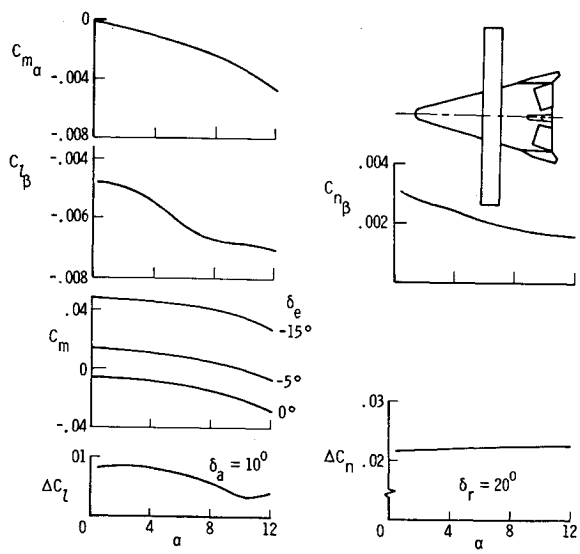

Fig. 3 Stability and control parameters—HL-10 with wing.